

## Properties of dune topographic state space for six barrier islands of the U.S. southeastern Atlantic coast

Jackie A. Monge and J. Anthony Stallins

Department of Geography, University of Kentucky, Lexington, KY, USA

### ABSTRACT

Barrier island dunes are postulated to exhibit two states, or stability domains. In this model, transitions between domains can exhibit irreversibility. However, these transitions may also be bistable, whereby the topography of either domain can develop at a location. To infer evidence for these dynamical properties and link them to dune topography, statistical mapping of dune topographic state space was undertaken for six barrier islands of the southeastern U.S. Atlantic coast. Topographies for three to four plots per island were constructed from airborne LiDAR data. Elevation in each was quantified in terms of descriptive statistics, spatial autocorrelation and landscape patch structure. The state space derived from ordination of these data was not primarily structured by the domain model. Instead, positive and negative relief defined the major axis of topographic variability. Only the plot topographies intermediate of these extremes in relief and contained within a smaller window of elevations resembled those of the two-state model. Their emergence along the second axis of variability was correlated with the spatial autocorrelation of elevation and geographic factors related to wave and tidal energy. Topographies suggestive of irreversibility and bistability were distinguishable based on their position in state space relative to these two domains regions.

### ARTICLE HISTORY

Received 5 March 2016

Accepted 3 August 2016

### KEYWORDS

Dunes; overwash;  
topography; state space;  
topology

## Introduction and rationale

Barrier islands protect coastal areas (Feagin et al., 2015; Otvos, 2012; Spalding et al., 2014; Temmerman et al., 2013). By filtering hydrodynamic and sedimentological influences originating from the sea, dune landforms protect the mainland from the full effects of tropical and extratropical storms. However, the processes responsible for the formation, maintenance and destruction of barrier islands are related to the evolution of smaller, superimposed features that include vegetated sand dunes (Keijsers, De Groot, & Riksen, 2016; Plant et al., 2014).

Many coastal scholars have emphasized the importance of dune topography and vegetation to the persistence of barrier island form and function (Davidson-Arnott, 2005; Everard, Jones, & Watts, 2010; Feagin et al., 2010; Vinent & Moore, 2013). The first classifications of barrier island coasts proposed two self-entailing process-form island morphologies. They

result from interactions among tidal range, wave energy, dune topography and vegetation responses to inundation and sediment burial (Davis & Hayes, 1984; Godfrey, 1977; Godfrey & Godfrey, 1973; Hayes, 1979). Microtidal barrier islands persist through low topographic profiles maintained in part by dune vegetation. The lateral rooting strategy of burial-tolerant grasses reduces vertical dune development and lowers resistance to the spread of overwash into back barrier habitats. On squat, drumstick-shaped mixed-energy mesotidal barrier islands, plant growth forms promote a rougher overwash-resisting ridge-and-swale topography. The geometry of these landforms tends to deflect overwash rather than promote its spread into back-barrier habitats. On both island morphologies, barrier functions are hypothesized to persist partly because the response of dune vegetation to the prevailing patterns of sediment mobility sets up biogeomorphic conditions that perpetuate vegetation and topography in a positive feedback. Although sediment budget, island orientation, antecedent geology and storm history can be constraining factors (Masselink & van Heteren, 2014; Psuty & Silveira, 2010), these landscape feedbacks can become preconditioned along coastal sectors (Morton & Sallenger, 2003).

Later studies distilled these ideas into a two-state model for barrier island dunes. Invoking the concept of stability domains from resilience theory (i.e. Gunderson, 2000), Stallins (2001, 2005) used plant functional abundances, the relationship between plant diversity and elevation, and the covariance of soil properties and vegetation to argue for the expression of stabilizing biogeomorphic feedbacks on two exemplars of barrier island morphological types, South Core Banks, North Carolina and Sapelo Island, Georgia. Wolner et al. (2013) and Brantley, Bissett, Young, Wolner, and Moore (2014) documented the distribution of topography-modifying dune grasses and historical overwash frequency to define analogous “high” (disturbance-resisting) and “low” (disturbance-reinforcing) barrier islands of the Virginia coast. From a more dynamical systems perspective (e.g. Scheffer, Carpenter, Dakos, & van Nes, 2015), Vinent and Moore (2015) and Goldstein and Moore (2016) numerically derived these states and designated them as a high “resistant-dune” state or a low “overwash-flat” state. By comparing modeling of dune biophysical parameters with dune elevation statistics derived from LiDAR, Vinent and Moore (2015) also detailed how either of the two domain states of barrier islands can develop where dune-constructing and erosional forces are balanced. Stretches of coast exemplifying this bistability can exhibit the topography of either domain. Goldstein and Moore (2016) substantiated the potential expression of three dune dynamical states: one or the other of the two stability domain states and bistability. Although terminology and methodological style vary according to the lineage of scholarship, the two-state stability domain model with bistability is the shared interpretation of the dynamical properties of barrier dunes.

Knowledge about the topographies associated with stability domains and bistable states is relevant to understanding how barrier coasts respond to storm forcings. Whether a stretch of barrier coast manifests the topographic characteristics of a stability domain or of a bistable state shapes what kinds of transitions to anticipate. Storm inputs may promote frequent transitions in topography along a bistable coast. Bistable locations may, in general, be more variable in time and across space because they cannot simultaneously reinforce and resist disturbance at a landscape scale (Kéfi et al., 2014; Stallins, 2005, p. 205). By contrast, under similar meteorological perturbations, coastal strands exhibiting stability domain topographies may persist until some threshold is reached. Then, topography may transition irreversibly to a new domain state. At present, it remains difficult to

differentiate states susceptible to non-catastrophic bistability versus irreversible regime changes (Kéfi et al., 2014).

Coastal geomorphologists have long articulated how dune topography along stretches of coast can vary in relation to similar kinds of underlying dynamics (Psuty & Silveira, 2010; Sherman & Bauer, 1993). To distinguish among the biogeomorphic dynamical properties associated with the two-state stability domain model and bistability, we compared dune topography for 22 sites among six barrier islands of the U.S. southeastern Atlantic coast. Topography was characterized by a suite of variables ranging from summary values like average elevation to more continuous, three-dimensional measures incorporating the spatial structure of elevation. To discriminate quantitatively among these topographies in terms of their propensity for bistability, for irreversibility, or for the reinforcing positive feedbacks of the domain states, we analyzed the structure, or topology (Donohue et al., 2013; Prager & Reiners, 2009) of these multivariate descriptors. While the topographic details of dunes and their landscape structure are implied as an important biogeomorphic component of the twofold classification of barrier island morphology, to the two-state stability domain model, and for bistability, they have not been fully incorporated as explanatory variables. Prior studies have emphasized single-point elevations, dune crest heights, isolated shore perpendicular topographic cross sections, and highly idealized shoreface geometries to infer dynamical properties at the expense of more complex spatial information that dune landforms express at multiple scales. Primary foredune height and the elevational change spanned by waves as they run up onto the beach do indeed convey the likelihood of overwash during storm forcings (Sallenger, 2000). However, given the capacity of dune plants to adapt to and modify dune surfaces (Vincent & Moore, 2013), the characterization of the fine-scale patterns of topography and landscape configuration of dune landforms (e.g. Houser, 2013; Long, de Bakker, & Plant, 2014; Sherman et al., 2013) may be necessary to distinguish among dune dynamical properties that relate to how dune biogeomorphic systems recover and reorganize in response to overwash forcing events. The spatial patterns of substrate conditions and vegetation in other systems have been shown to be linked to domain dynamics and bistability (Scheffer et al., 2009, p. 56).

## Analytical context

To infer the dynamical properties among barrier dunes, we performed statistical mapping. In statistical mapping, real-world observations are arranged in relation to each other based on properties other than location. Distance between observations or sampling locations in a statistical map reflects similarity in attributes like elevation, surface roughness and patch shape rather than kilometers or meters of on-the-ground intervening distance. When entities become represented in mathematical spaces in this way, it can help elucidate underlying properties and mechanisms (Prager & Reiners, 2009). The statistical mapping of geomorphological or ecological observations demarcates their state space, the occupied to less-occupied conditions under which they manifest (see examples in Baas & Nield, 2010; Inkpen & Hall, 2016; Murray & Paola, 1996). State space establishes the range of circumstances for a dynamic phenomenon to develop, from those that are favored and more likely, to those that are less persistent and unlikely to occur. The positions of observations in this state space can then be used to identify and infer where dynamical processes and forms are operative. Where observations cluster, for example, can indicate a more dynamically preferred state.

Empty regions in state space suggest the presence of thresholds or combinations of conditions and structural features that are unlikely to develop or persist.

Baas and Nield (2010) used cellular automata to model the state space for dune landform-vegetation interactions. Two types of vegetation (pioneer grasses and later successional woody shrubs) in association with different aeolian sediment transport conditions produced nine different landform states. Less spatially explicit modeling by Bel and Ashkenazy (2014) identified three categories of dune landforms based on the interaction of aeolian sediment mobility and dune vegetation. Using one-dimensional modeling, Goldstein and Moore (2016) mathematically derived three regions in barrier dune state space corresponding to the two-state stability domain model plus bistability. In this study, we rely upon dune elevational observations derived from airborne coastal LiDAR. These data facilitated a comparison of what is permissible in a numerical model or simulation with what is actually observed over large extents of real-world conditions. Remote sensing is a strategy advocated by Scheffer et al. (2015, p. 163) for inferring the properties of dynamical systems. Baas and Nield (2010) also endorsed how remotely sensed data sets provide the twin advantages of breadth and detail needed to infer the dynamical properties of state space.

The value of this exploratory, observation-driven statistical mapping of dune topographic state space is that it compares recent modeling insights with those derived from an explicitly geographical framework. Such approaches to mapping and data visualization can be used to refine hypotheses and develop new ones (Prager & Reiners, 2009; Sagarin & Pauchard, 2009). But to avoid affirming the consequent (Cushman, 2010, p. 37), a weakness of exploratory studies, we referenced our LiDAR-derived state space to a graphical model that fuses recent theoretical perspectives on the generic architecture of dynamical systems (Kéfi et al., 2014; Pace, Carpenter, & Cole, 2015; Scheffer et al., 2015) with the twofold domain model plus bistability (Figure 1(a) and (b)).

In this model, transitions in dune state space may be gradual and reversible, with little to no bistability or threshold-driven abrupt change (Figure 1(a)). At other locations, bistability may be fully expressed, along with more irreversible threshold-driven transitions (Figure 1(b)). Irreversibility implies that transitions to the other state occur under different sets of circumstances. The trajectories of development shift abruptly at different points along a gradient of controlling resources and conditions. A return to a former state is possible, but due to the threshold nature of the transition, it can occur only along a different trajectory and with different inputs. Irreversibility in this sense denotes hysteresis (Scheffer, Carpenter, Foley, Folke, & Walker, 2001; van Nes & Scheffer, 2005). For hysteresis to develop, the conditions shaping the expression of domains must overlap. Depending upon position in state space relative to this overlap in conditions, transitions between domains may follow irreversible trajectories versus more bistable tracks (Figure 1(b)).

Temporal studies have provided the bulk of evidence for the current general understanding of dynamical properties in ecological systems. However, it is increasingly recognized that there is a spatial component of their expression (Bel, Hagberg, & Meron, 2012; Dakos, Carpenter, van Nes, & Scheffer, 2015; Dakos, van Nes, Donangelo, Fort, & Scheffer, 2010; Scheffer & van Nes, 2007). Stretches of coast may flip from one domain to another over time. However, these flips in time will have also involved the local spatial contagion of biogeomorphic processes and forms. Small domains of the alternative domain may form within the same island. Thus, as Scheffer et al. (2015) posed, the question about dynamical

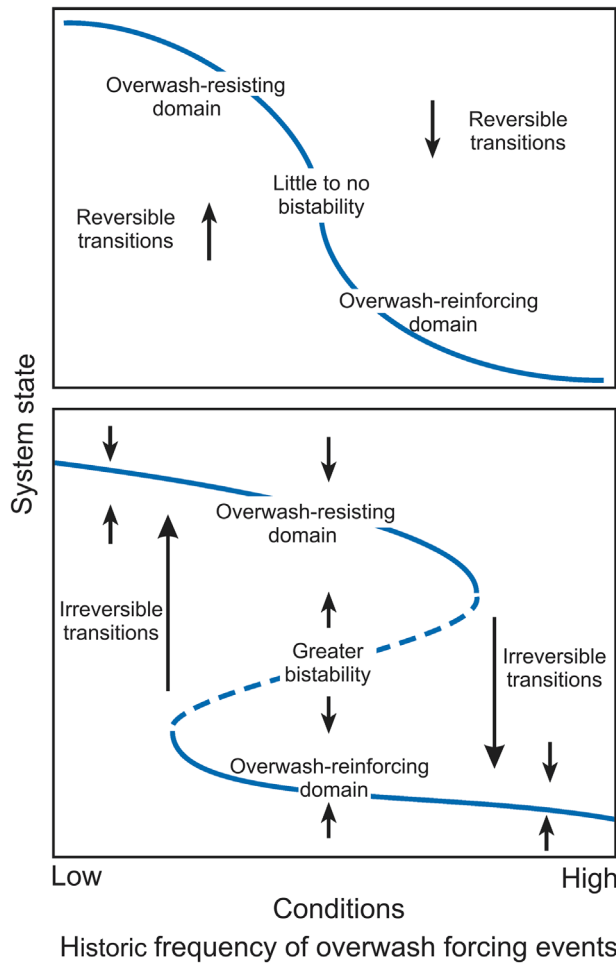


**Figure 1.** Dynamical properties that may develop across barrier island dunes. Source: Line art adapted from Scheffer et al. (2015).

Notes: Arrows indicate the direction in which a system tends to develop in response to domain feedbacks. In the upper panel, transitions within domains and between domains are more gradual and reversible. There is less bistability. As the curve becomes folded in the lower panel, there is overlap in the conditions characterizing domains. The region of overlap (represented by the dashed line) is less likely to confer persistence of barrier functions. Hence, there is more bistability. Outside of this bistable middle region, there is a greater propensity for irreversible transitions, (i.e. hysteresis). Longer arrows reflect the larger distance in state space spanned by these irreversible transitions.

systems is not only about when transitions occur, but also where and in what way they manifest characteristics indicative of domain feedbacks, bistability, or irreversibility.

To formalize how position in dune topographic state space reflects these dynamical properties, we posed the initial question: (1) what is the dominant source of topographic variability in barrier dune state space? This question sought to clarify if barrier dune state space is dominantly structured by the twofold domain model or by another source of variability. This permits the identification of the major boundary conditions and the general properties of state space. Next, (2) is there evidence in state space for topographies that exhibit domain feedbacks, bistability, or irreversible transitions? Since domain states are dynamically favored, more densely occupied regions of state space signal their manifestation.

Overlap in some of the topographic conditions defining domain states would be a precursor for the expression of bistability and irreversibility. Regions of state space where this overlap occurs may be sparsely occupied given they would reflect dynamically unfavorable topographies intermediate of both domains. Topographies with the propensity for bistability should develop in proximity to this region. Conversely, a greater separation of plots from the same island across the dynamically unfavorable region between domains suggests threshold transitions and irreversibility. In sum, the distances separating plots of a barrier island in state space (a reflection of their topographic similarity), and their location in this state space relative to the sources of variance structuring it, allow topographies to be associated with their potential dynamical properties. Lastly, our state space mapping permits an assessment of (3) how variable are the topographies expressed on any particular barrier island? Across all the scalar extents and resolutions on a single island there would be innumerable configurations of topography. But how do dune topographies and their dynamical properties, when expressed at distances relevant to coastal planning – that is, at the scale of one or a few kilometers – vary on an individual island?

It is important to emphasize that our characterization of dune topographic state space does not depend upon a space-for-time substitution. Our state space approach provides an indication of the topographies that occur in reality and those that do not. Occupied areas represent topographies that minimize several functional problems. They do not need to represent an evolutionary or developmental stage but rather the range of forms that can be taken given variations in constraining properties (Inkpen & Hall, 2016). The most frequent forms represent the most common outcome. However, other forms nearby could represent slightly different interactions between constraining properties that do not necessarily have to be developmentally related. In this study, domain states, irreversibility and bistability are inferred as a function of occupancy and position in topographic state space rather than as an arrangement of alongshore topographic contrasts that unproblematically correspond to a developmental sequence in time.

In addition, the nomenclature and criteria for identifying barrier islands are complex and not entirely free of debate (Otvos, 2010). We retain the usage of the term *barrier island*, when it may be broadly accurate to consider them as *barrier-related landforms* since some may be spits or barrier beaches (Leatherman, 1978). In addition, we did not discriminate between the mode of origin of dunes, as seen in the contrasts between beach ridges and foredunes (Hesp, 2011). Whether foredunes were incipient or established (Hesp, 2002) was less important than the overall pattern of elevations composing dune topography. Dunes in this study have a landscape functional role (Arkema et al., 2013). While we did not directly measure the biological properties of the dune surface, the dynamical properties of dunes are strongly correlated with vegetation and biogenic crusts (Hayden, Santos, Shao, & Kochel, 1995; Kinast, Meron, Yizhaq, & Ashkenazy, 2013; Vinent & Moore, 2013).

## Study area and methods

Six islands were selected based on how well they minimized (but did not eliminate) human impacts and how they maximized contrasts in coastal setting along the U.S. southeast Atlantic coast (Figure 2). Google Earth and digital aerial orthophotos were used to visually identify stretches of distinctive beach and dunes (e.g. Houser, 2009; Sherman & Bauer, 1993) to sample within each of these six islands. In general, these stretches corresponded

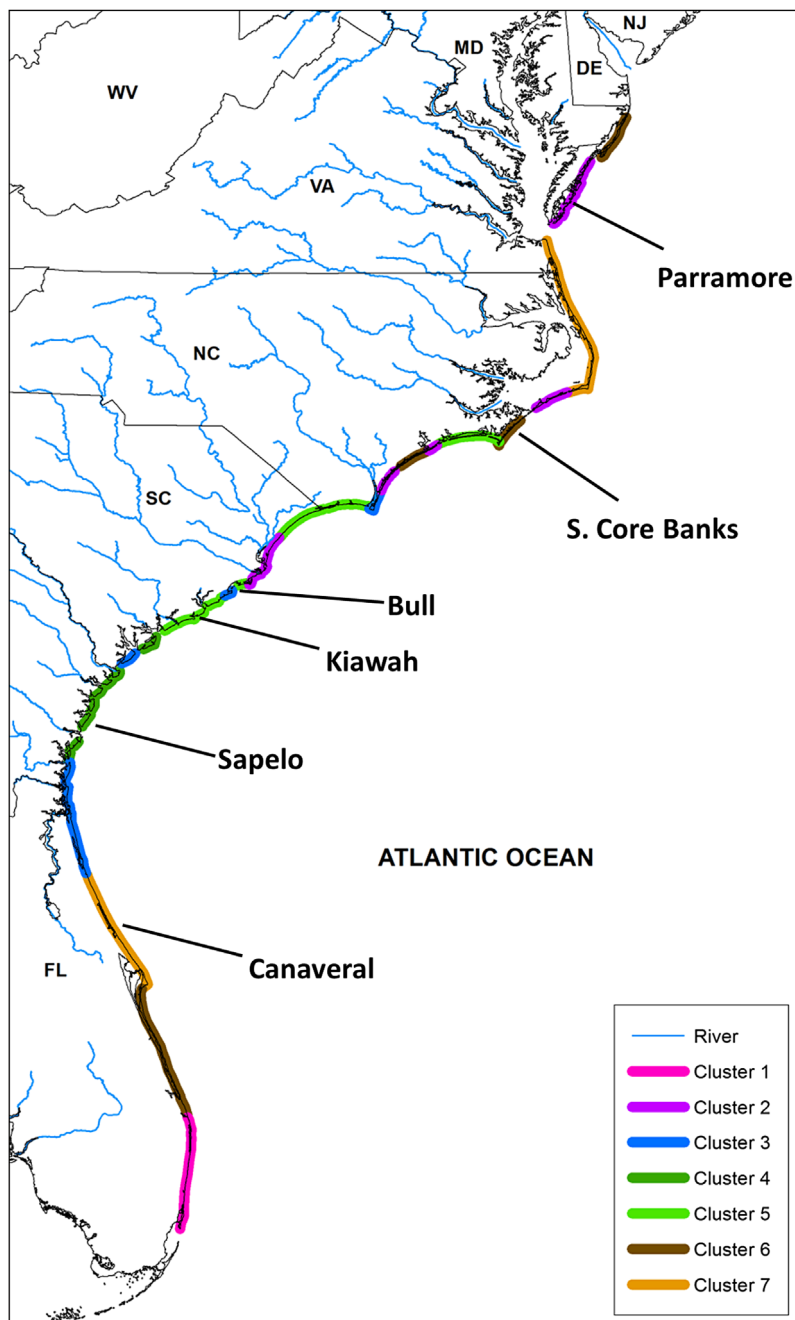


**Figure 2.** Morphological clusters of the six barrier islands selected for this study. Source: Data for classification derived from Google Earth, U.S. Geological Survey's Coastal Vulnerability Index database (Gornitz, Daniels, White, & Birdwell, 1994; Hammar-Klose & Thieler, 2001), and historical hurricane track data (1851–2012) made available by NOAA Coastal Services. Cluster 1 island in South Florida had extensive human impacts and was not included in the construction of state space.

Notes: Each island belongs to a distinctive barrier island morphology as derived from a hierarchical clustering of mean island width, length, mean tidal range, mean wave height, compass orientation and number of tropical storm/hurricane strikes.

to where the beaches were wide or narrow and where the dominant geomorphic conditions varied from accretional to erosional. Next, a single square plot was randomly located within each distinctive stretch of beach and dune topography. Instead of standardizing the size of all plots, the distance extending inland from below the waterline to the first occurrence of extensive dense woody vegetation or salt marsh defined the initial length of a side of the rectangular plot. This shore perpendicular distance was then used as the length of all the other sides.

Each island required three or four of these plots to capture the range of its dominant beach and dune topographic contrasts, resulting in a total of 22 plots. The northernmost island in this study, Parramore Island (four dune plots), is a transgressive, tidal-dominated barrier located on the Delmarva Peninsula of Virginia. Parramore is rapidly retreating toward the mainland at short-term rates of approximately 2.7 m/yr (Richardson & McBride, 2007). Bull Island (four plots) is a mixed-energy barrier located on the coast of South Carolina north of Charleston. Sapelo Island (three plots) is a mixed-energy barrier approximately halfway between Savannah, Georgia and Jacksonville, Florida. Dune LiDAR sampling here was confined to the small Holocene island welded to the larger Pleistocene core often identified as Sapelo. Kiawah Island (four plots) is a mixed-energy barrier in South Carolina south of Charleston. South Core Banks (three plots) is a transgressive, wave-dominated barrier located in North Carolina. It is the most extensive of the three islands that make up the Core Banks island chain. Landward rates of retreat are approximately 1.5 m/year (Riggs & Ames, 2007). Cape Canaveral (four plots) is a wave-dominated barrier located on the central coast of Florida.

Digital elevation models were constructed for each plot using LiDAR ground elevation data available online through NOAA's Coastal Services Center. A 2010 data-set collected by the United States Army Corps of Engineers was used for four of the six islands. For this data-set, the vertical (horizontal) accuracy was 15 cm (75 cm) and nominal point space was 2 m. Due to small gaps in the 2010 LiDAR coverage, plot topographies for South Core Banks and Parramore Island were constructed from post-Sandy LiDAR data sets collected by the U.S. Geological Survey in 2012. For these data, vertical (horizontal) accuracy was 7.5 cm (19.4 cm) and nominal point space was 1 m. Because topography varies according to storm climate (Riggs & Ames, 2007), these post-storm data still represent the historic range of variability in topography. Leaving out post-storm events would similarly influence characterization of dune state space by downweighting the topographic signature of storm forcings in favor of quiescent conditions.

LiDAR point elevations for each plot were resampled to a resolution of 1 m and then interpolated using inverse distance weighing to fill any gaps. LiDAR processing was performed in ArcGIS using LAStools. The North American datum for each plot was referenced to the mean high water mark using VDatum (National Oceanic & Atmospheric Administration & National Ocean Service [NOAA/NOS], 2012). The plots were then clipped along the edge coinciding with the MHW mark elevation of zero, resized to be square, and rotated to a common orientation. This reduced the plot down to its final pre-analysis dimensions. By characterizing and analyzing topography in plots of different size, we follow Jackson and Fahrig's (2014) recommendation that environmental sampling be conservatively large whenever possible. In a natural sampling design, the phenomena under study define the observational window. Plot size became a spatial characteristic of the sampled topographies and was retained as an explanatory variable.

We developed three sets of variables to characterize topography. Each set captured a distinctive aspect of elevation and topography. This insured the incorporation of topographic details that might be missed if only one type of variable or one level of measurement were used. The first set of variables consisted of absolute levels of measurement comprising descriptive statistics for elevations in each plot (mean, maximum, mode, 25th percentile and 75th percentile elevations). To quantify the explicitly spatial character of elevation with relativized measures (i.e. those not expressed in terms of meters), our second set of variables was derived from the spatial autocorrelation structure of point elevations in each plot (see Turner, Gardner, & O'Neill, 2001, p. 129). For each island plot, Moran's *I* was calculated for distance lags at 1-m intervals in a direction perpendicular to the shoreline. Moran's *I* ranges from +1 (strong positive autocorrelation) to -1 (strong negative correlation). GS+ software (Robertson, 2000) was employed to calculate Moran's *I* and to construct directional correlograms. Information about the size (in meters) of each plot was retained in these correlograms.

Since the directional correlograms did not convey the shore-parallel variability in dune topography that also shapes responses to high water events (Houser, 2013; Sherman et al., 2013). FRAGSTATS software (McGarigal, Cushman, & Ene, 2012) was used to generate a third set of dune metrics representing the three-dimensional landscape patch structure of elevation (e.g. Ryu & Sherman, 2014). Because FRAGSTATS is designed to work with categorical observations, LiDAR data points for each plot were converted into a categorical representation by rasterizing unique elevation values and then reclassifying pixels into elevation intervals. This decreased the number of elevation classes from all the possible centimeter intervals (essentially a continuous surface representation), to one based approximately on decimeter intervals (a categorically oriented representation). To avoid derivation of FRAGSTATS descriptors lacking a process interpretation (Kupfer, 2012), we initially chose landscape indices identified by Cushman, McGarigal, and Neel (2008) as having consistent ecologically meaningful value. This set of indices was then constrained to those well suited for characterizing continuous surfaces like elevation (McGarigal, Tagil, & Cushman, 2009) and for discerning pattern-process relationships associated with foredune building and overwash. We selected three indices: the perimeter-area fractal dimension (PAFRAC), the area-weighted mean shape index (SHAPE\_AM) and the aggregation index (AI).

These three sets of variables were merged into one composite data-set of plot-level dune metrics. However, correlogram data were not reducible to a single numerical plot-level value like the elevation statistics or FRAGSTAT indices. To merge these data it was first necessary to employ principal coordinates analysis (PCoA), a distance-based, non-parametric counterpart to principal components analysis, to reduce Moran's *I* values for each plot's correlogram down to principal (*x* and *y*) axis coordinates. One of the primary uses of ordination is data dimensionality reduction. Ordination is also a tool for visualizing and inferring the properties of dynamical systems (Andersen, Carstensen, Hernandez-Garcia, & Duarte, 2009; Angeler et al., 2015; Baas & Nield, 2007, 2010). PCoA was utilized again to derive the multivariate statistical map needed to infer the dynamical relationships among different regions of dune topographic state space. PCoA maximized the extraction of variance in the plot-level composite data-set onto the first and then succeeding axes. The position of plots in this statistical map reflected the axis coordinates assigned to them in PCoA. Smaller intervening distances between plots in this state space indicated greater topographic similarity. Although plot position reflects the joint influence of all the dune metrics, the relative

influence of individual variables in particular regions of state space was inferred through Spearman's non-parametric correlations ( $r_s$ ) of PCoA axis coordinates with plot-level dune metrics. Monte Carlo randomizations of the observed data were used to derive the significance of PCoA axes and hence the number of axes to retain. All variables were relativized to their standard deviates before ordination. Euclidean distance was selected as the distance metric. PCoA was performed in PC-ORD V 6.12 software (McCune & Mefford, 2011).

## Results

### *Plot elevations and topography*

Plot sizes ranged from  $215 \times 215$  m on South Core Banks to  $40 \times 40$  m on the north end of Cape Canaveral. The highest elevations, as well as the greatest elevation range, were on Cape Canaveral (Figure 3). Parramore Island had the overall lower elevations and narrower elevational range. The correlogram data (Figure 4) reduced down to two significant principal components based on Monte Carlo randomizations of the data, capturing 75% of the variance (Axis 1 = 63%,  $p = 0.001$ ; Axis 2 = 12%,  $p = 0.001$ ). Plots on the negative end of the dominant first PCoA ( $x$ ) axis exhibited correlograms like those of South Core A, where strong positive correlations at small distance classes changed to strong negative correlations at larger distance classes. Positive positions on the first axis resembled the spatial autocorrelation structure shown for Sapelo A. For these, initially positive correlations among

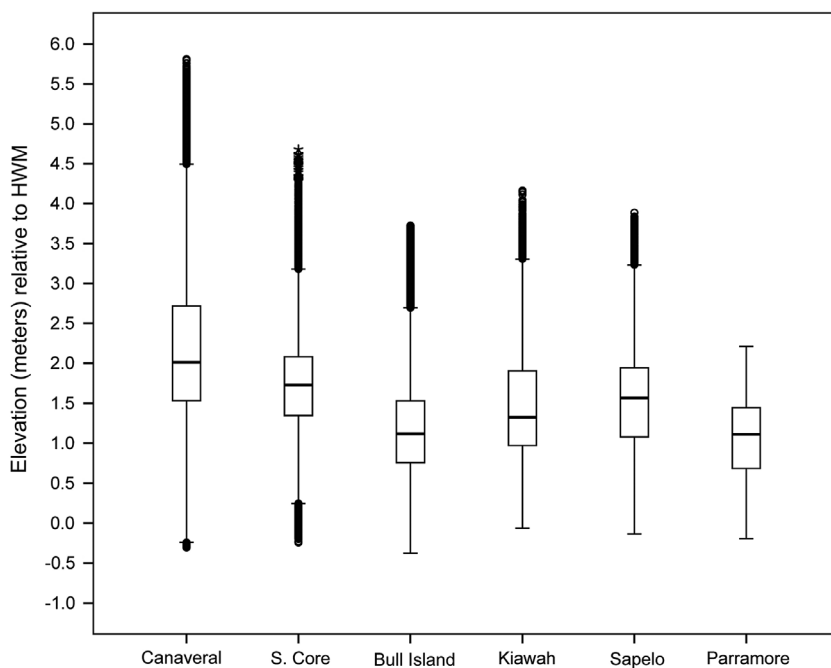


**Figure 3.** Box plots of elevation distribution (in meters) for each island relative to the mean high water tidal datum.

Notes: Line in the middle of the boxes is the median, lower box edge represents 25th percentile, top box hinge is the 75th percentile. Whiskers denote maximum and minimum elevation values within  $1.5 \times$  of the interquartile range. Outliers lie beyond these values.

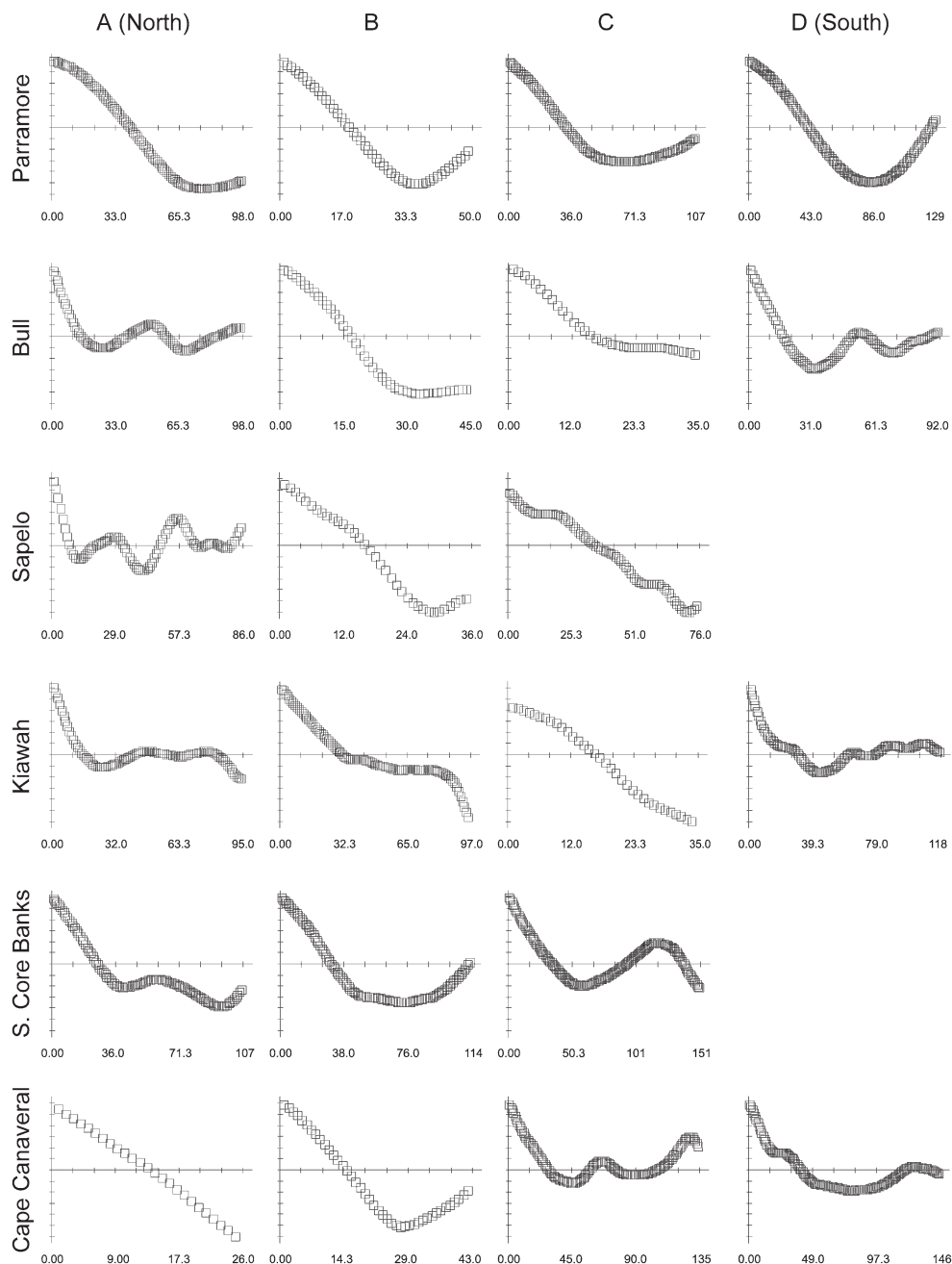


**Figure 4.** Shore-perpendicular directional correlograms for elevation at 1-m distance lags up to the length of the plot.

Notes: X-axis is in meters. Y axis ranges from +1 to -1.

elevations became uncorrelated at larger distance classes. FRAGSTATS indices responded to the range of patch configurations between islands, from linear dune topographies to more circular elevation patch structure where overwash was common (Figure 5). Only two

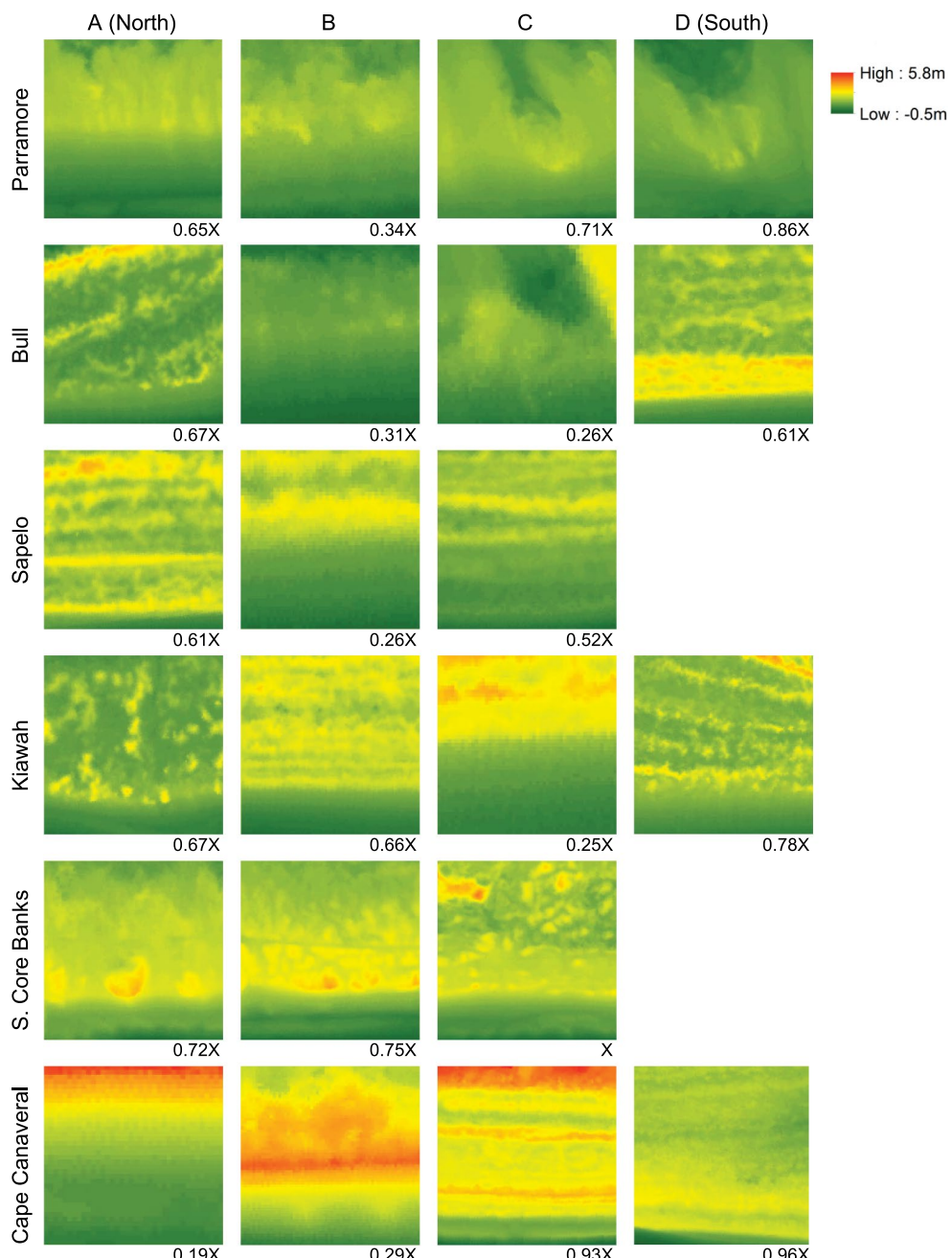


**Figure 5.** Digital elevation models and plot size before reclassification to decimeter categorical intervals and analysis in FRAGSTATS.

Notes: Letters indicate position along island, from A (northernmost) to D (southernmost). Island plots differed in size although scaled to be the same here. Conversion factors below each raster can be used to derive their dimensions relative to the largest island plot, South Core Banks C (215 m by 215 m). For example, the actual dimensions of plot C on Sapelo are 112 m by 112 m ( $0.52 \times 215 \text{ m} = 111.8 \text{ m}$ ).

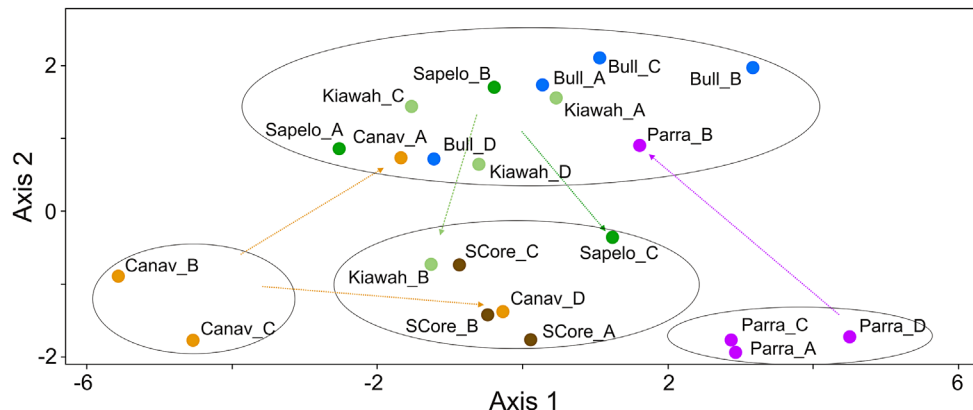


**Figure 6.** PCoA scatterplot of dune topography state space.

Notes: Axes are scaled in relation to the variance extracted (Axis 1 = 57%; Axis 2 = 22%). Both axes were significantly different from Monte Carlo randomizations of the data ( $p < 0.05$ ). Dashed colored lines are individual island plots whose position in state space shifted away from the domain where the majority of their plots fell. Units on axis reflect similarity based on Euclidean distance.

of the ten dune variables had statistically significant correlations ( $p < 0.05$ ) with plot size, the  $x$  coordinate for the reduced correlogram data ( $r_s = 0.69$ ), and SHAPE\_AM ( $r_s = 0.79$ ).

### PCoA state space

The PCoA of the final composite data-set (descriptive statistics, reduced correlogram  $x$  and  $y$  coordinates, and FRAGSTATS indices) captured 77% of the variability in dune topography on two significant axes (Axis 1 = 57%,  $p = 0.001$ ; Axis 2 = 22%,  $p = 0.03$ ; Figure 6). The greater amount of topographic variability along the first axis corresponded to the high to low dunes of Cape Canaveral and Parramore, respectively. Plots for these islands formed outlying clusters at opposite regions of the first axis.

The second PCoA axis separated island plots into what resembled overwash-reinforcing and overwash-resisting stability domains. Plots from the mostly mixed-energy mesotidal barrier islands of Bull, Sapelo and Kiawah clustered together at one end of the second axis. Plots for the microtidal barrier island of South Core Banks clustered at the other end. However, these two domain regions in state space did not always contain the full suite of plots for any individual island. Canaveral A and D, Parramore B, Sapelo C and Kiawah B were all located in state space at a distance away from the rest of their respective island plots. This implies that some islands contained topographies that were more similar to those found at more distant coastal locations. Canaveral D (FL), for example, was more similar to the topographies found on South Core Banks (NC) than its within-island neighbors. Some islands had plots that occurred in both stability domain regions delineated by the second axis. For example, plot C on the overwash-resisting mixed-energy barrier island Sapelo, had a topography more like that of overwash-reinforcing microtidal barrier islands.

### PCoA axis correlations

Correlations of first PCoA axis plot position with the elevation statistics confirmed that high, constructive positive relief and lower, potentially more erosional relief form the major axis of variability for dune state space (Figure 7(a)–(e)). Mean elevation had a statistically significant high positive correlation with plot position along the first axis ( $r_s = -0.88$ ). From left to right on the first axis, higher and less likely to be overwashed plots gave way to lower elevation plots where overwash could be expected to be more frequent (Figure 7(a) and (b)). This strong correlation emerged largely as a consequence of the high and low elevations for plots on Canaveral and Parramore, respectively.

FRAGSTATS indices supported this interpretation. The aggregation index (AI) had a strong significant correlation with the first PCoA axis ( $r_s = 0.81$ ). AI measures how aggregated adjacent elevation observations are to each other. Changes in AI along the first axis indicated changes among plots in the patch size of similarly ranged elevations (Figure 7(c)). Large patch sizes, such as those for Parramore Island, form when frequent overwash aggregates and homogenizes elevation. SHAPE\_AM, the mean shape index, was also significantly correlated with the first axis ( $r_s = 0.66$ ). More positive plot positions along the first axis for this index imply a greater irregularity in patch shape, as would be expected with increasing overwash (Figure 7(d)). The negative direction was associated with a greater abundance of rectilinear, shore-parallel foredunes suggestive of decreasing inland overwash penetration. PAFRAC expresses the fractal dimension of a landscape. Variability in this index signals differences in the underlying pattern-process relationship. The correlation of PAFRAC with first axis ( $r_s = -0.67$ ) corroborated that this axis tracks changes in the relative importance of processes related to dune building versus topography-simplifying overwash (Figure 7(e)). Plot size was not correlated with the first PCoA axis.

The second PCoA state space axis had weak correlations with elevational descriptive statistics and FRAGSTATS indices. Instead, plot position along the second axis was significantly correlated with the x coordinate from the reduced correlogram data (Figure 7(f);  $r_s = 0.72$ ). There was also a moderate but statistically significant negative correlation of plot size with the second PCoA axis ( $r_s = -0.64$ ). The predominantly mixed-energy mesotidal barrier island plots in the positive direction on the second axis tended to have spatially uncorrelated elevations at increasing distance classes and smaller plot sizes, as exemplified by Sapelo A. The predominantly microtidal barrier island plots in the negative direction on the second axis tended to have larger plot sizes and stronger negative spatial autocorrelations of elevations at longer distance classes, as exemplified by South Core A. While correlations were, overall, fewer and weaker along the second axis, and the variance extracted on it was a third of that extracted on the first axis, its inclusion delineated state space regions resembling overwash-reinforcing and overwash-resisting domain states based in part on geographic location.

### Discussion

Overwash-reinforcing and overwash-resisting domain topographies were not the major source of variability in barrier dune state space. As expressed on the first PCoA axis, the greatest source of variance spanned high to low relief. Extremes in dune elevation, from Canaveral B and C at high elevations to Parramore D at lower elevations (Figure 8(a)–(b))

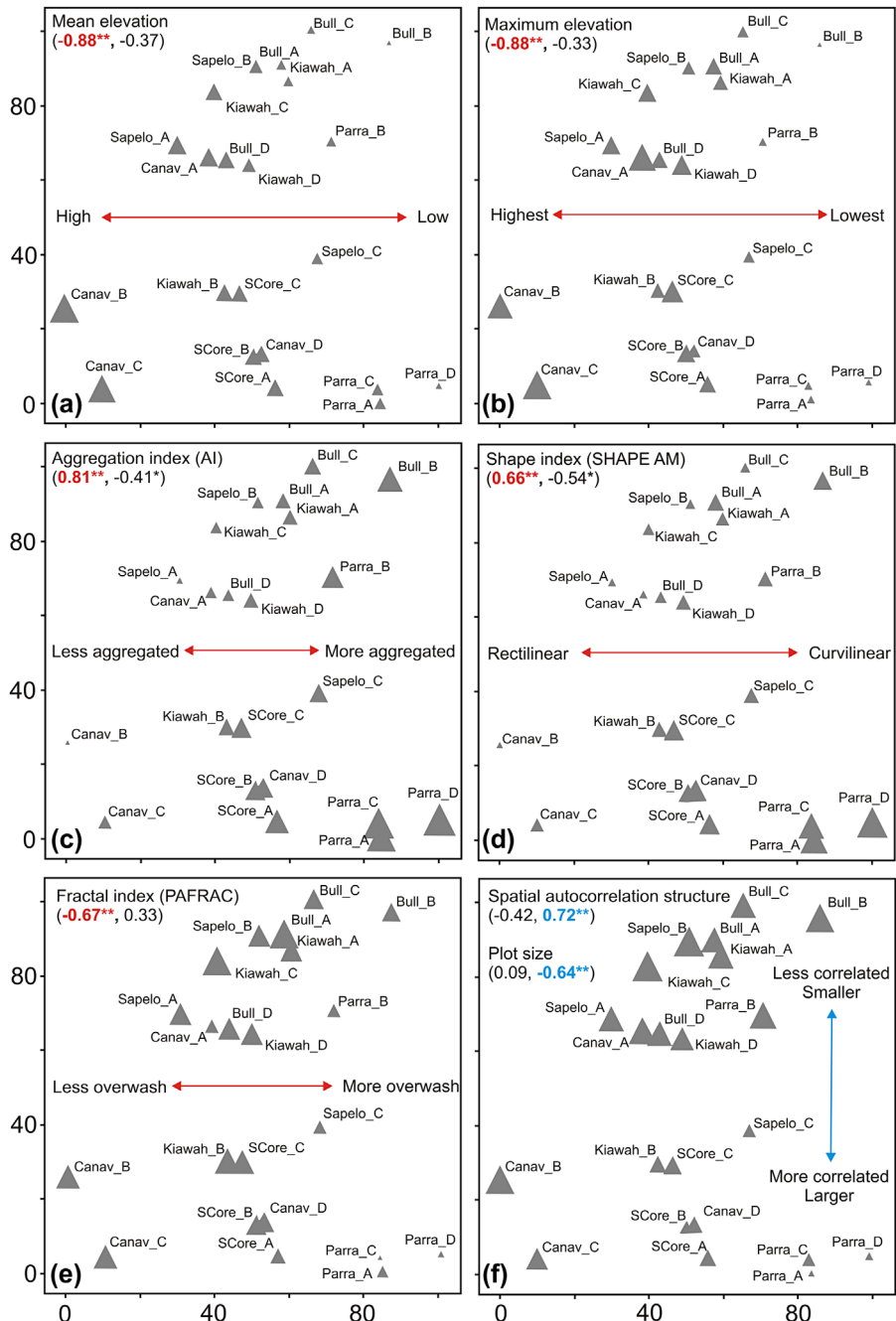


**Figure 7.** Individual dune variables having strong statistically significant Spearman's correlation coefficients with PCoA axes.

Notes: Each island plot is represented by a triangle scaled in size to match the observed value of the variable. Units of Euclidean distance along each axis have been rescaled to 0–100. \* $p < 0.05$ ; \*\* $p < 0.001$ .

defined the boundary conditions of state space. Statistically significant correlations of FRAGSTATS indices and elevational statistics with first-axis plot position additionally

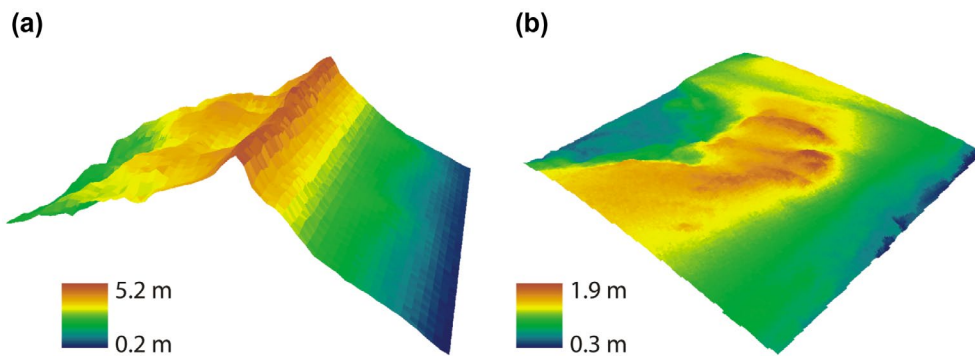


**Figure 8.** Topographies representing the major axis of variability in dune state space. Vertical scale is exaggerated. (a) Single high fronting positive dune relief of plot B on Cape Canaveral; plot size =  $62 \times 62$  m. (b) Low, negative relief of plot D on Parramore Island; plot size =  $184 \times 84$  m.

confirmed that positive and negative relief, along with the constructive versus degradational processes accompanying them, are the major source of variability in barrier dune state space.

The feedbacks that define the two-domain model do not appear likely to establish at these upper and lower elevational limits. Where positive relief is high, as on Canaveral B, biogeomorphic feedbacks would be less directly coupled to maritime inputs. Instead of the stabilizing vegetation-overwash feedbacks of the domain model, the more proximate controls may be aeolian sediment transport, vegetation density and local topographically-mediated climatic and hydrological factors. With increasing positive relief, topographic resistance to overwash may allow late successional woody shrubs to colonize behind the dunes. These shrubs can outcompete burial-tolerant grasses needed in the landscape to maintain the potential for dune recovery after overwash (e.g. Odum, Smith, & Dolan, 1987; Zinnert et al., 2016). Similarly, where elevation becomes extremely low, topographic highs result from the erosional removal of sediments. These residual landforms are exemplified by the “pimples” of Parramore Island (Figure 9(a) and (b)), a term invoked by Hayden et al. (1995). Although dunes are by definition depositional, sediments around them can also be eroded to form this negative, or inverted relief. Low elevation dunes and pimples may preempt establishment of the biogeomorphic feedbacks between overwash and topography that can develop in stability domains (Roman & Nordstrom, 1988).

The separation of plots into what resembled stability domains occurred only when the second PCoA axis was included (Figure 10(a) and (b)). These two domain states differed in how their elevations were spatially autocorrelated and in the width of the dunes, as expressed as plot size. Yet these domains were not homogenous in terms of island affinities. Canaveral A and D, Parramore B, Sapelo C and Kiawah B appeared in regions of state space distant from where majority of their island’s plots fell. Inspection of air photos for these plots confirmed their distinctiveness from adjoining dunes. Sapelo C is a low-lying accretional area subject to overwash on a mesotidal island where overwash is typically infrequent. Aerial photography indicates woody vegetation extends close to the shore for Parramore B. Island retreat into woody vegetation here may contribute to scarping and development of an overwash-resisting topography on an otherwise frequently overwashed island. Canaveral A and D are located at either end of an island with a pronounced change in orientation near its mid-point. Kiawah B is in an area with private beach residences. This location has

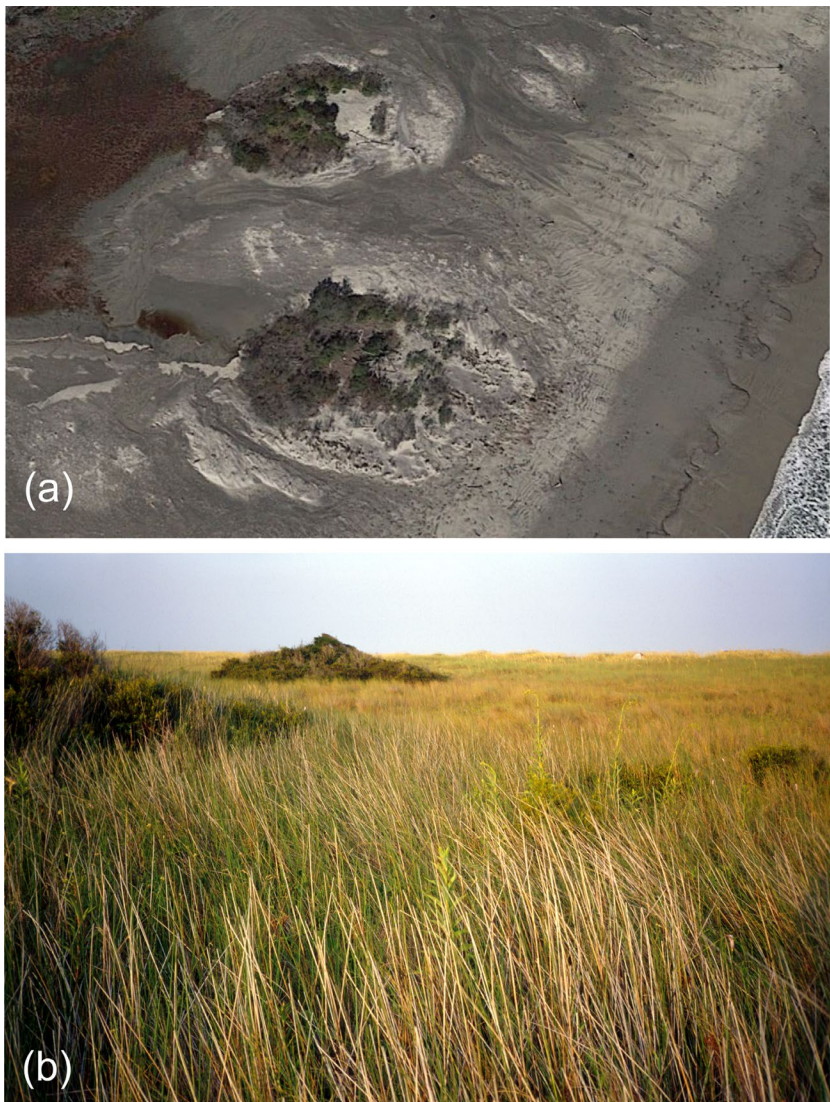


**Figure 9.** (a) Examples of negative relief: the pimples of Parramore Island (photo from Google Earth). (b) Pimples that developed on a frequently overwashed site on South Core Banks, North Carolina (Photo by J.A. Stallins).

a relatively broad flat dune topography that resembles South Core Banks. The appearance of this topography here could be natural or a result of localized anthropogenic impacts that have altered topography and exposure to overwash (e.g. Rogers et al., 2015). These shifts in the position of island plots in state space convey that local within-island coastal context can deviate from the larger geographic controls of tidal and wave energy to the extent that a plot's topography can more closely resemble that of a distant island.

Changes in spatial autocorrelation have been shown to indicate transitions in dynamical properties (Dakos et al., 2010; Scheffer et al., 2009; Scheffer et al., 2012). As observed in this study, differences in plot spatial autocorrelation structure along the second axis of dune state

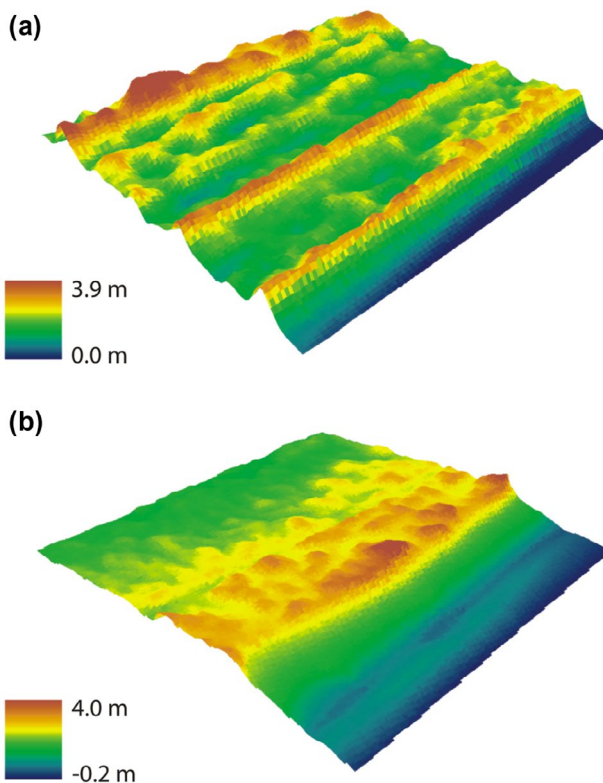


**Figure 10.** Representative domain topographies expressed along the second axis in state space. Vertical scale is exaggerated. (a) Sapelo A, an example of the overwash-resisting domain; plot size = 111 × 111 m. (b) South Core Banks B, an example of the overwash-reinforcing domain; plot size = 161 × 161 m.  
Note: See Figure 5 for all plot sizes.

space were associated with the separation of stability domains. Overlap in the conditions shared by domains was also detected. Where both domain states were distributed along the second axis corresponded to a range of elevations (approximately  $1.0 \pm 0.5$  m relative to the HMW) along the middle of the first axis. Following Vinent and Moore (2015), this central region of our state space may correspond to where dune constructing and erosional forces approach a balance. Here, the affinity of a plot for one domain or another may be less a reflection of the absolute value of elevation and more related to geographic context and spatial autocorrelation structure of these elevations. In other words, the local relative dominance of microtidal versus mesotidal coastal conditions and the continuous spatial structure of dune elevation, rather than any absolute value for height above the high water mark, may be better predictors of emergence of domain feedbacks and their respective topographies.

Domain states may be unlikely to develop above or below this overlapping range of elevation, insofar as the span of islands sampled in this study constrains our results. Elevations may be either too high or too low for the integration of feedbacks between dune topography, overwash and vegetation. We thus propose that there are two additional regions of topographic state space to complement the existing twofold domain model plus bistability: a region of high, positive relief dunes with strong resistance to overwash but little

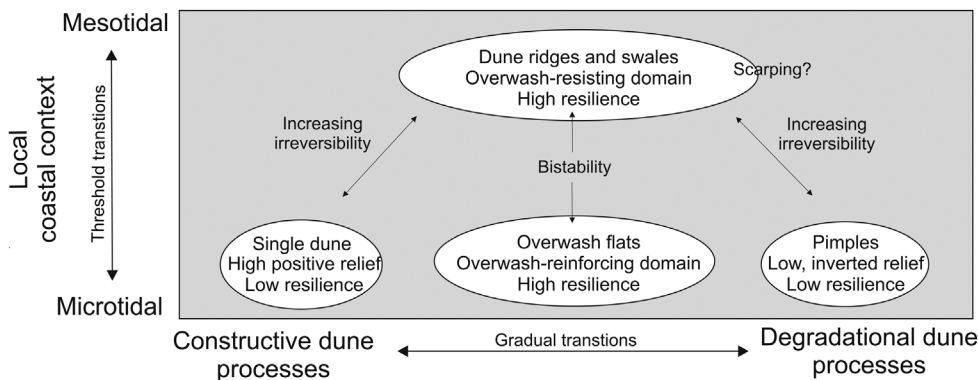


**Figure 11.** Dune topographic state space.

Notes: Ellipses are regions of state space occupied by topographic observations in this study. Intervening gray-shaded regions represent less occupied regions of state space. Arrows indicate propensity for affinity for bistable, irreversible and gradual change.

biogeomorphic capacity to recover if overtopped, and a region with low dunes and inverted topography that has little resistance to overwash and weak resilience-generating biogeomorphic feedbacks (e.g. Hayden et al., 1995; Odum et al., 1987).

Plots positioned within this range of elevations along the first axis but also on the interior cusps of domains may define topographies with a propensity for bistability. The positions of Sapelo C and Kiawah B suggest that they may possess topographic characteristics of both domains and thus a greater potential for bistability. By contrast, the Canaveral A and Parramore B plots occurred in the domain opposite of the one in which the majority of their plots fell. Their larger separation in state space across domains on the second axis also encompassed greater changes in elevation and landscape patch structure expressed along the first axis. These two plots may represent topographies that have undergone more irreversible transitions. To revert back to the other domain may require a change in inputs involving wave energy and sediment mobilization greater than what would be required in bistable regions of state space. Still, not all islands had plots that exhibited bistability or irreversible transitions. South Core Banks and Bull Island plots had positions in only one domain. The differences in topography among plots of these islands may indicate more gradational, reversible transitions, with less propensity for bistability and irreversibility.

## Conclusion

Based on the topographic properties associated with the dominant axes of variability in our state space, the relative occupancy of some regions in state space over others, and the distances among plots from the same island, we inferred relationships between topography and their dynamical properties. In response to our first question, we found that the extremes of positive and negative relief were the largest source of variability in dune state space. The expression of the two-state domain model appears to occur only within a smaller range of elevations contained by these boundary conditions (Figure 11). Within this window of elevations, spatial autocorrelation may be a more responsive indicator of how local deviations from the broader microtidal-mesotidal coastal context give rise to domain topographies.

High positive or low negative relief outside of this window may represent regions of occupancy in state space that are less likely to reinforce their persistence through biogeomorphic feedbacks coupled to the overwash forcing regime.

The second of our three questions sought to infer evidence for topographies indicative of bistability and irreversibility. The potential for bistability and irreversible transitions between these domains was inferred by the development of a relatively unoccupied region in the center of state space. Individual plots in this region are likely to exhibit topographies intermediate of both domains and thus have propensity for bistability. The topographies of island plots that fell in both domains and spanned larger changes in elevation and its patch structure may be more indicative of transitions within an island that are more irreversible. In response our third question, these aforementioned shifts in the position of plots in state space convey how within-island variability in dune topography, at kilometer-scale stretches of coast, is a better focus for coastal planning and management than entire islands. Plot position in state space can vary widely for a single island.

As LiDAR data sets are now widely available, it is feasible to map out the dune state space for a larger number of barrier islands. LiDAR data sets from multiple years could also be analyzed to extend state space into the temporal dimension. The properties ascribed to dune state space could also be tested by including islands with human-altered dunes (Grafals-Soto, 2012; Jackson & Nordstrom, 2011; Martinez, Gallego-Fernandez, Garcia-Franco, Moctezuma, & Jimenez, 2006). Dune plots from heavily modified barrier islands could be expected to plot in or near the unstable region of state space or at other outlier locations because they have been shaped by human impacts into idiosyncratic topographic process-form relationships. Structure-from-motion photography derived from drones, kites, or paint pole-mounted cameras can also be used to rapidly acquire high-resolution elevation data. It is likely that facets of this state space would change with the inclusion of more islands, but its overall variance structure should have some consistency. However, increases in the dimensionality of state space accompanying a greater number of islands and plots would require visualization methods other than PCoA. Networks, for example, may be able to work around the issue of having to use mathematically constrained orthogonal axes to represent the topographic relationships among plots.

There also remains the need to link vegetation to dune topographic state space so as to infer more about underlying biogeomorphic and ecological mechanisms. Topography is in part a signature of vegetation (Corenblit et al., 2015; Phillips, 2016; Vincent & Moore, 2013). Dune plant functional types (e.g. Ciccarelli, 2015) and biogenic crusts (e.g. Kinast et al., 2013; Viles, Naylor, Carter, & Chaput, 2008) contribute to the dynamical properties of dune state space. In flume experiments, dune vegetation has been shown to reduce net erosion on the dune face, regardless of the wave conditions, the morphology of the beach-dune profile, or the mode of erosion (Silva, Martínez, Odériz, Mendoza, & Feagin, 2016).

In sum, a comparison of LiDAR-derived topographies with an inherent vegetation signature confirmed the existing two-domain state plus bistability model of barrier dunes. However, two other dynamical regions in topographic state space were identified. High single-fronting dunes or low-elevation dune coasts with a potential for inverted relief also constitute regions in state space. It is valid that the elevation of the beach and the fronting dunes constrain overwash occurrence (Sallenger, 2000). However, data summarizing local topographic details as well as the landscape-scale geometry of dune systems, under realistic exposures to biotic modification, may help detect the range of dynamical properties on

barrier dunes. To the extent that dune topography and species compositions could be simultaneously mapped in state space, management might then skillfully mimic landscape-scale biogeomorphic modification to retain desired barrier functions instead of relying on hard engineering practices (Feagin et al., 2010, 2015; Nordstrom et al., 2011).

## Disclosure statement

No potential conflict of interest was reported by the authors.

## References

- Andersen, T., Carstensen, J., Hernandez-Garcia, E., & Duarte, C. M. (2009). Ecological thresholds and regime shifts: Approaches to identification. *Trends in Ecology & Evolution*, 24, 49–57.
- Angeler, D. G., Allen, C. R., Garmestani, A. S., Gunderson, L. H., Hjerne, O., & Winder, M. (2015). Quantifying the adaptive cycle. *PLoS ONE*, 10, e0146053.
- Arkema, K. K., Guannel, G., Verutes, G., Wood, S. A., Guerry, A., Ruckelshaus, M., & Silver, J. M. (2013). Coastal habitats shield people and property from sea-level rise and storms. *Nature Climate Change*, 3, 913–918.
- Baas, A. C. W., & Nield, J. M. (2007). Modelling vegetated dune landscapes. *Geophysical Research Letters*, 34(6), 1–5.
- Baas, A. C. W., & Nield, J. M. (2010). Ecogeomorphic state variables and phase-space construction for quantifying the evolution of vegetated aeolian landscapes. *Earth Surface Processes and Landforms*, 35, 717–731.
- Bel, G., & Ashkenazy, Y. (2014). The effects of psammophilous plants on sand dune dynamics. *Journal of Geophysical Research: Earth Surface*, 119, 1636–1650.
- Bel, G., Hagberg, A., & Meron, E. (2012). Gradual regime shifts in spatially extended ecosystems. *Theoretical Ecology*, 5, 591–604.
- Brantley, S. T., Bissett, S. N., Young, D. R., Wolner, C. W., & Moore, L. J. (2014). Barrier island morphology and sediment characteristics affect the recovery of dune building grasses following storm-induced overwash. *PLoS ONE*, 9, e104747.
- Ciccarelli, D. (2015). Mediterranean coastal dune vegetation: Are disturbance and stress the key selective forces that drive the psammophilous succession? *Estuarine, Coastal and Shelf Science*, 165, 247–253.
- Corenblit, D., Baas, A., Balke, T., Bouma, T., Fromard, F., Garfano-Gómez, V., ... Julien, F. (2015). Engineer pioneer plants respond to and affect geomorphic constraints similarly along water-terrestrial interfaces world-wide. *Global Ecology and Biogeography*, 24, 1363–1376.
- Cushman, S. A. (2010). Space and time in ecology: Noise or fundamental driver? In S. A. Cushman & F. Huettmann (Eds.), *Spatial complexity, informatics, and wildlife conservation* (pp. 19–41). Tokyo: Springer.
- Cushman, S. A., McGarigal, K., & Neel, M. C. (2008). Parsimony in landscape metrics: Strength, universality, and consistency. *Ecological Indicators*, 8, 691–703.
- Dakos, V., Carpenter, S. R., van Nes, E. H., & Scheffer, M. (2015). Resilience indicators: Prospects and limitations for early warnings of regime shifts. *Philosophical Transactions of the Royal Society of London B: Biological Sciences*, 370, 20130263.
- Dakos, V., van Nes, E. H., Donangelo, R., Fort, H., & Scheffer, M. (2010). Spatial correlation as leading indicator of catastrophic shifts. *Theoretical Ecology*, 3, 163–174.
- Davidson-Arnott, R. G. D. (2005). Conceptual model of the effects of sea level rise on sandy coasts. *Journal of Coastal Research*, 21, 1166–1172.
- Davis, R. A., & Hayes, M. O. (1984). What is a wave-dominated coast? *Marine Geology*, 60, 313–329.
- Donohue, I., Petchey, O. L., Montoya, J. M., Jackson, A. L., McNally, L., Viana, M., & Emmerson, M. C. (2013). On the dimensionality of ecological stability. *Ecology Letters*, 16, 421–429.

- Everard, M., Jones, L., & Watts, B. (2010). Have we neglected the societal importance of sand dunes? An ecosystem services perspective. *Aquatic Conservation: Marine and Freshwater Ecosystems*, 20, 476–487.
- Feagin, R. A., Figlus, J., Zinnert, J. C., Sigren, J., Martínez, M. L., Silva, R., & Carter, G. (2015). Going with the flow or against the grain? The promise of vegetation for protecting beaches, dunes, and barrier islands from erosion. *Frontiers in Ecology and the Environment*, 13, 203–210.
- Feagin, R. A., Smith, W. K., Psuty, N. P., Young, D. R., Martinez, M. L., Carter, G. A., & Koske, R. E. (2010). Barrier Islands: Coupling Anthropogenic Stability with Ecological Sustainability. *Journal of Coastal Research*, 26, 987–992.
- Godfrey, P. J. (1977). Climate, plant response and development of dunes on barrier beaches along the United States East Coast. *International Journal of Biometeorology*, 21, 203–216.
- Godfrey, P., & Godfrey, M. M. (1973). Comparison of ecological and geomorphic interactions between altered and unaltered barrier island systems in North Carolina. In D. R. Coates (Ed.), *Coastal Geomorphology* (pp. 239–258). New York: State University of New York.
- Goldstein, E. B., & Moore, L. J. (2016). Stability and bistability in a one-dimensional model of coastal foredune height. *Journal of Geophysical Research: Earth Surface*, 121, 964–977.
- Gornitz, V. M., Daniels, R. C., White, T. W., & Birdwell, K. R. (1994). The development of a coastal risk assessment database: Vulnerability to sea-level rise in the US Southeast. *Journal of Coastal Research*, Special Issue No. 12, 327–338.
- Grafals-Soto, R. (2012). Effects of sand fences on coastal dune vegetation distribution. *Geomorphology*, 145, 45–55.
- Gunderson, L. H. (2000). Ecological resilience – In theory and application. *Annual Review of Ecology and Systematics*, 31, 425–439.
- Hammar-Klose, E. S., & Thieler, E. R. (2001). *Coastal vulnerability to sea-level rise: A preliminary database for the U.S. Atlantic, Pacific and Gulf of Mexico coasts*. Retrieved July 22, 2015, from <http://pubs.usgs.gov/dds/dds68/>
- Hayden, B. P., Santos, M. C. F. V., Shao, G. F., & Kochel, R. C. (1995). Geomorphological controls on coastal vegetation at the Virginia Coast Reserve. *Geomorphology*, 13, 283–300.
- Hayes, M. O. (1979). Barrier island morphology as a function of tidal and wave regime. In S. P. Leatherman (Ed.), *Barrier islands from the Gulf of St. Lawrence to the Gulf of Mexico* (pp. 1–27). New York, NY: Academic Press.
- Hesp, P. (2002). Foredunes and blowouts: Initiation, geomorphology and dynamics. *Geomorphology*, 48, 245–268.
- Hesp, P. (2011). Dune coasts. In W. Eric & M. Donald (Eds.), *Treatise on estuarine and coastal science* (pp. 193–221). Waltham, MA: Academic Press.
- Houser, C. (2009). Synchronization of transport and supply in beach-dune interaction. *Progress in Physical Geography*, 33, 733–746.
- Houser, C. (2013). Alongshore variation in the morphology of coastal dunes: Implications for storm response. *Geomorphology*, 199, 48–61.
- Inkpen, R., & Hall, K. (2016). Using morphospaces to understand tafoni development. *Geomorphology*, 261, 193–199.
- Jackson, H. B., & Fahrig, L. (2014). Are ecologists conducting research at the optimal scale? *Global Ecology and Biogeography*, 24, 52–63.
- Jackson, N. L., & Nordstrom, K. F. (2011). Aeolian sediment transport and landforms in managed coastal systems: A review. *Aeolian Research*, 3, 181–196.
- Kéfi, S., Guttau, V., Brock, W. A., Carpenter, S. R., Ellison, A. M., Livina, V. N., & Dakos, V. (2014). Early warning signals of ecological transitions: Methods for spatial patterns. *PLoS ONE*, 9, e92097.
- Keijser, J., De Groot, A., & Riksen, M. (2016). Modeling the biogeomorphic evolution of coastal dunes in response to climate change. *Journal of Geophysical Research: Earth Surface*, 121, 1161–1181.
- Kinast, S., Meron, E., Yizhaq, H., & Ashkenazy, Y. (2013). Biogenic crust dynamics on sand dunes. *Physical Review E*, 87, 020701.
- Kupfer, J. A. (2012). Landscape ecology and biogeography: Rethinking landscape metrics in a post-FRAGSTATS landscape. *Progress in Physical Geography*, 36, 400–420.

- Leatherman, S. P. (1978). *Barrier islands from the Gulf of St. Lawrence to the Gulf of Mexico*. New York, NY: Academic Press.
- Long, J. W., de Bakker, A. T. M., & Plant, N. G. (2014). Scaling coastal dune elevation changes across storm-impact regimes. *Geophysical Research Letters*, 41, 2899–2906.
- Martinez, M. L., Gallego-Fernandez, J. B., Garcia-Franco, J. G., Moctezuma, C., & Jimenez, C. D. (2006). Assessment of coastal dune vulnerability to natural and anthropogenic disturbances along the Gulf of Mexico. *Environmental Conservation*, 33, 109–117.
- Masselink, G., & van Heteren, S. (2014). Response of wave-dominated and mixed-energy barriers to storms. *Marine Geology*, 352, 321–347.
- McCune, B., & M. J. Mefford. (2011). PC-ORD. Multivariate analysis of ecological data. Version 6.12. MjM Software, Gleneden Beach, OR.
- McGarigal, K., Cushman, S. A., & Ene, E. (2012). FRAGSTATS v4: Spatial pattern analysis program for categorical and continuous maps. University of Massachusetts at Amherst, MA. Retrieved from <http://www.umass.edu/landeco/research/fragstats/fragstats.html>
- McGarigal, K., Tagil, S., & Cushman, S. A. (2009). Surface metrics: An alternative to patch metrics for the quantification of landscape structure. *Landscape Ecology*, 24, 433–450.
- Morton, R. A., & Sallenger, A. H., Jr. (2003). Morphological impacts of extreme storms on sandy beaches and barriers. *Journal of Coastal Research*, 19, 560–573.
- Murray, A. B., & Paola, C. (1996). A new quantitative test of geomorphic models, applied to a model of braided streams. *Water Resources Research*, 32, 2579–2587.
- National Oceanic and Atmospheric Administration and National Ocean Service. (2012). *Vertical datum transformation: Integrating America's elevation data*. VDatum: Vertical Datums Transformation. Retrieved July 22, 2015, from <http://vdatum.noaa.gov/>
- Nordstrom, K. F., Jackson, N. L., Kraus, N. C., Kana, T. W., Bearce, R., Bocamazo, L. M., & De Butts, H. A. (2011). Enhancing geomorphic and biologic functions and values on backshores and dunes of developed shores: A review of opportunities and constraints. *Environmental Conservation*, 38, 288–302.
- Odum, W. E., Smith, T. J., III, & Dolan, R. (1987). Suppression of natural disturbance: Long-term ecological change on the outer banks of North Carolina. In M. Turner (Ed.), *Landscape heterogeneity and disturbance* (pp. 123–135). New York, NY: Springer.
- Otvos, E. G. (2010). Definition of barrier islands: Discussion of Pilkey, O. H., Cooper, J. A. G., & Lewis, D. A. (2009), Global distribution and geomorphology of fetch-limited barrier islands, *Journal of Coastal Research*, 25(4), 819–837. *Journal of Coastal Research*, 26, 787.
- Otvos, E. G. (2012). Coastal barriers – Nomenclature, processes, and classification issues. *Geomorphology*, 139, 39–52.
- Pace, M. L., Carpenter, S. R., & Cole, J. J. (2015). With and without warning: Managing ecosystems in a changing world. *Frontiers in Ecology and the Environment*, 13, 460–467.
- Phillips, J. D. (2016). Landforms as extended composite phenotypes. *Earth Surface Processes and Landforms*, 41, 16–26.
- Plant, N. G., Flocks, J., Stockdon, H. F., Long, J. W., Guy, K., Thompson, D. M., ... Dalyander, P. S. (2014). Predictions of barrier island berm evolution in a time-varying storm climatology. *Journal of Geophysical Research-Earth Surface*, 119, 300–316.
- Prager, S. D., & Reiners, W. A. (2009). Historical and emerging practices in ecological topology. *Ecological Complexity*, 6, 160–171.
- Psuty, N. P., & Silveira, T. M. (2010). Global climate change: An opportunity for coastal dunes? *Journal of Coastal Conservation*, 14, 153–160.
- Richardson, T. M., & McBride, R. A. (2007). *Historical shoreline changes and morphodynamics of Parramore Island, Virginia (1852–2006)*. Coastal Sediments '07, New Orleans, LA.
- Riggs, S. R., & Ames, D. (2007). *Effect of storms on Barrier Island dynamics, core banks, Cape Lookout National Seashore, North Carolina, 1960–2001*. United States Geological Survey Scientific Investigations Report 2006–5309. Reston, VA: U.S. Department of the Interior, U.S. Geological Survey.
- Robertson, G. P. (2000). GS+: *Geostatistics for the environmental sciences*. Plainwell, MI: Gamma Design Software.

- Rogers, L. J., Moore, L. J., Goldstein, E. B., Hein, C. J., Lorenzo-Trueba, J., & Ashton, A. D. (2015). Anthropogenic controls on overwash deposition: Evidence and consequences. *Journal of Geophysical Research: Earth Surface*, 120, 2609–2624.
- Roman, C. T., & Nordstrom, K. F. (1988). The effect of erosion rate on vegetation patterns of an east coast barrier island. *Estuarine, Coastal and Shelf Science*, 26, 233–242.
- Ryu, W., & Sherman, D. J. (2014). Foredune texture: Landscape metrics and climate. *Annals of the Association of American Geographers*, 104, 903–921.
- Sagarin, R., & Pauchard, A. (2009). Observational approaches in ecology open new ground in a changing world. *Frontiers in Ecology and the Environment*, 8, 379–386.
- Sallenger, A. H. (2000). Storm impact scale for barrier islands. *Journal of Coastal Research*, 16, 890–895.
- Scheffer, M., Bascompte, J., Brock, W. A., Brovkin, V., Carpenter, S. R., Dakos, V., & Sugihara, G. (2009). Early-warning signals for critical transitions. *Nature*, 461, 53–59.
- Scheffer, M., Carpenter, S. R., Dakos, V., & van Nes, E. H. (2015). Generic indicators of ecological resilience: Inferring the chance of a critical transition. *Annual Review of Ecology, Evolution, and Systematics*, 46, 145–167.
- Scheffer, M., Carpenter, S., Foley, J. A., Folke, C., & Walker, B. (2001). Catastrophic shifts in ecosystems. *Nature*, 413, 591–596.
- Scheffer, M., Carpenter, S. R., Lenton, T. M., Bascompte, J., Brock, W., Dakos, V., & Van Nes, E. H. (2012). Anticipating critical transitions. *Science*, 338, 344–348.
- Scheffer, M., & van Nes, E. H. (2007). Shallow lakes theory revisited: Various alternative regimes driven by climate, nutrients, depth and lake size. *Hydrobiologia*, 584, 455–466. doi: [10.1007/s10750-007-0616-7](https://doi.org/10.1007/s10750-007-0616-7)
- Sherman, D. J., & Bauer, B. O. (1993). Dynamics of beach-dune systems. *Progress in Physical Geography*, 17, 413–447.
- Sherman, D. J., Hales, B. U., Potts, M. K., Ellis, J. T., Liu, H. X., & Houser, C. (2013). Impacts of Hurricane Ike on the beaches of the Bolivar Peninsula, TX, USA. *Geomorphology*, 199, 62–81.
- Silva, R., Martínez, M., Odériz, I., Mendoza, E., & Feagin, R. (2016). Response of vegetated dune-beach systems to storm conditions. *Coastal Engineering*, 109, 53–62.
- Spalding, M. D., McIvor, A. L., Beck, M. W., Koch, E. W., Möller, I., Reed, D. J., & Woodroffe, C. D. (2014). Coastal ecosystems: A critical element of risk reduction. *Conservation Letters*, 7, 293–301.
- Stallins, J. A. (2001). Soil and vegetation patterns in barrier-island dune environments. *Physical Geography*, 22, 79–98.
- Stallins, J. A. (2005). Stability domains in barrier island dune systems. *Ecological Complexity*, 2, 410–430.
- Temmerman, S., Meire, P., Bouma, T. J., Herman, P. M. J., Ysebaert, T., & De Vriend, H. J. (2013). Ecosystem-based coastal defence in the face of global change. *Nature*, 504, 79–83.
- Turner, M. G., Gardner, R. H., & O'Neill, R. V. (2001). *Landscape ecology in theory and practice*. New York, NY: Springer.
- van Nes, E. H., & Scheffer, M. (2005). Implications of spatial heterogeneity for catastrophic regime shifts in ecosystems. *Ecology*, 86, 1797–1807.
- Viles, H. A., Naylor, L. A., Carter, N. E. A., & Chaput, D. (2008). Biogeomorphological disturbance regimes: Progress in linking ecological and geomorphological systems. *Earth Surface Processes and Landforms*, 33, 1419–1435.
- Vincent, O. D., & Moore, L. J. (2013). Vegetation controls on the maximum size of coastal dunes. *Proceedings of the National Academy of Sciences of the United States of America*, 110, 17217–17222.
- Vincent, O. D., & Moore, L. J. (2015). Barrier island bistability induced by biophysical interactions. *Nature Climate Change*, 5, 158–162.
- Wolner, C. W., Moore, L. J., Young, D. R., Brantley, S. T., Bissett, S. N., & McBride, R. A. (2013). Ecomorphodynamic feedbacks and barrier island response to disturbance: Insights from the Virginia Barrier Islands, Mid-Atlantic Bight, USA. *Geomorphology*, 199, 115–128.
- Zinnert, J. C., Shiflett, S. A., Via, S., Bissett, S., Dows, B., Manley, P., & Young, D. R. (2016). Spatial-temporal dynamics in barrier island upland vegetation: The overlooked coastal landscape. *Ecosystems*, 19, 685–697.